

HRTEM Study of nano-TiO₂ Powder

IONELA CARAZEANU POPOVICI^{1*}, MIHAI GIRTU², ELISABETA CHIRILA¹, VICTOR CIUPINA², GABRIEL PRODAN²

¹ Ovidius University, Chemistry Department, 124 Mamaia Blvd., 900527 Constanta, Romania,

² Ovidius University, Electron Microscopy Laboratory, 124 Mamaia Blvd., 900527 Constanta, Romania

Titanium dioxide (TiO₂) has been one of the most attractive photo electrochemical and photovoltaic material during the last decades due to its scientific and technological importance. The TiO₂ powder was synthesized by thermal hydrolysis of TiCl₄. The crystalline structures and morphologies of the powder have been characterized by high-resolution transmission electron microscopy (HRTEM) and X-ray diffraction (XRD). The crystals dimensions varied from 15 nm to 23 nm and it have been established that the studied nanopowder is stable in the anatase phase.

Keywords: TiO₂, anatase, nanoparticle, XRD, SEM, HRTEM, SAED

Since the early 1970s, there has been immense interest on the photochemistry of semiconductors, because of their beneficial features relating to the photocatalytic decontamination of water and air. A variety of semiconductor materials have been developed, such as Fe₂O₃, WO₃, ZnO and TiO₂. Due to its stability, nontoxicity, and broadly defined goal of efficiently detoxifying hazardous organic pollutants, TiO₂ has been studied extensively over the last two decades [1-6].

TiO₂ has many properties that make it very useful in different domains. As a result of the low position of the valence band (i.e. an energy gap between valence band (BV) and conduction band (BC) of about 3.2 eV has an excellent chemical stability. This makes it useful in the applications in chemically aggressive environments as a native oxide layer, which can protect the metal against corrosion. However, the well-known application of TiO₂ is as white pigment in paints. The combination of its refractive index with sufficiently small particle size results in a very efficient light scattering over a large wavelength range. Other important optical applications are its use as UV absorber in cosmetic products (such a sun cream) and as a transparent UV barrier in the food packaging industry.

At room temperature TiO₂ occurs in three natural forms: rutile, anatase and brookite. In the figure 1 the polymorphs forms of TiO₂ are presented.

So far, practical applications have been limited to the anatase and rutile forms which are most easily produced and seem to have the most interesting properties. Since rutile has a larger refractive index than anatase it is generally preferred in optical applications (anti-reflection coatings). Most of anatase - based applications are relatively new and are often based on a combination of

optical, chemical and electrical properties. Anatase has a higher electron mobility, and (photo) catalytic activity due to a more open structure than rutile. For these reasons anatase is used in dye-sensitized solar cells, wastewater purification reactors, lithium ions batteries, and electro - chromic windows. TiO₂ is presently widely used as a transparent n-type semiconductor in solar cells. The photo-response of TiO₂ in combination with different p-type materials is the subject for many investigations [7 - 20].

This paper presents the morphology and size characterization of titania particles synthesized by thermal hydrolysis of TiCl₄ in a mixed solvent of ethanol and water.

Experimental part

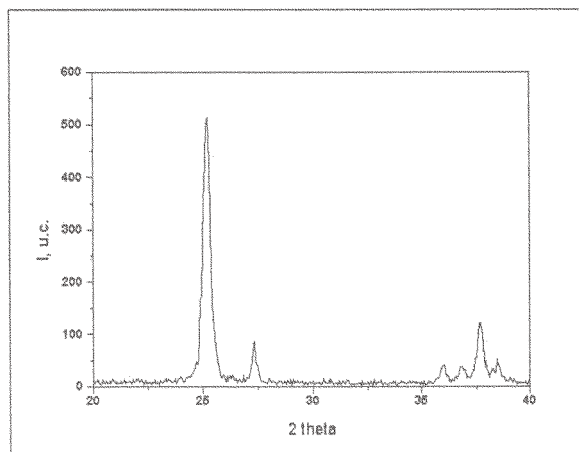
The TiO₂ powder was synthesized by thermal hydrolysis of TiCl₄ in a mixed solvent of ethanol and water. The synthesized TiO₂ powder was characterized by XRD. X-ray diffraction experiments were performed on a Shimadzu 6000 automatic diffractometer equipped with a graphite monochromator and CuK_α radiation ($\lambda = 1.5406\text{\AA}$, the scanning region 2θ was equal to $20 - 80^\circ$). The chemical composition of sample was studied using EDX investigations. Microstructural investigation of synthesized powders was performed using scanning electron microscopy (SEM) with Jeol JMS 5800 L electron microscope. The samples were coated with gold and examined in the as-fired condition, i.e., without polishing.

High-resolution transmission electron microscopy (HRTEM) was used to evaluate the purity and the phase composition of TiO₂ powder. The bright field - transmission electron microscopy (BF-TEM) investigations was performed with an electron microscope (model CM 120 ST manufactured by Philips) operating at 100 kV and

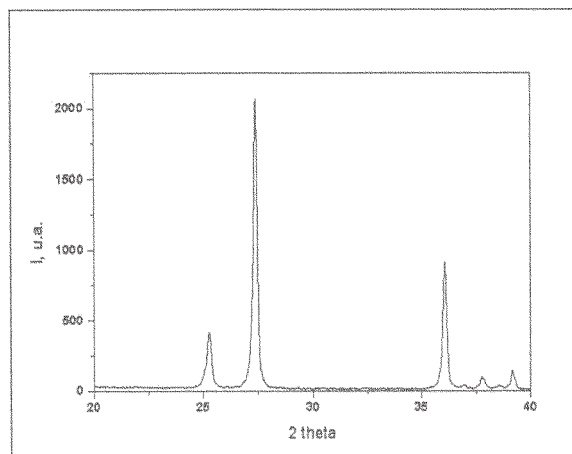


Fig. 1 The polymorphs forms of TiO₂: a) rutile; b) anatase; c) brookite

* email: icarazeanu@univ-ovidius.ro



(a)



(b)

Fig. 2 XRD patterns of the TiO_2 after heat treatment at: (a) 600°C; (b) 800°C

magnification maxim 1200000x. The resolution obtained in our cases was about 2Å. Lattice plane images give information about crystal structure and selected area electron diffraction (SAED) images help us to identify the phase. Also the crystals size distribution was studied.

Results and Discussions

Figure 2 shows the X-ray diffraction patterns of TiO_2 precursor and the corresponding titania samples.

The samples obtained by annealing at 600 and 800°C are assigned to the amorphous anatase (JCPDS File No. 21-1272) and rutile phase (JCPDS File No. 21-1276) of titania [23]. From the XRD pattern, the phase transition from anatase to rutile seems to occur at temperatures around 750 – 800°C, where the diffraction peaks of both phases are detected in the sample.

The chemical composition of sample was evaluated using EDX spectra and the figure 3 shows that the sample has Ti (59.78%) and O (39.89%).

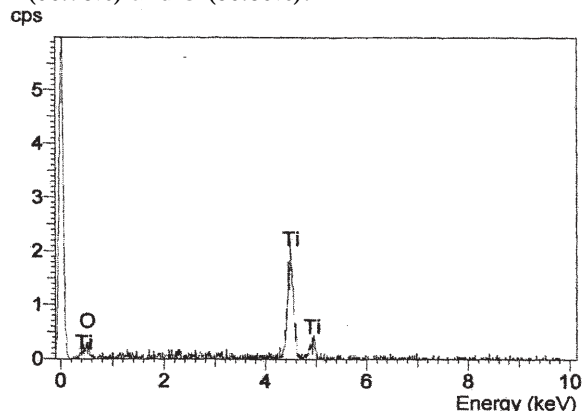
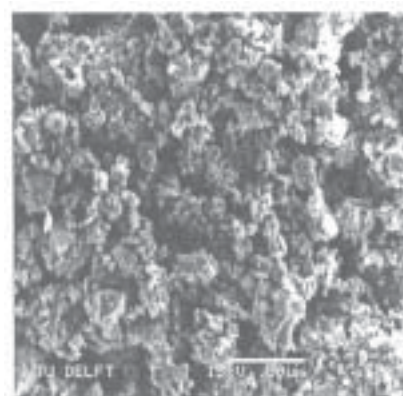


Fig. 3. EDX spectra for TiO_2 powder sample obtained at 500°C

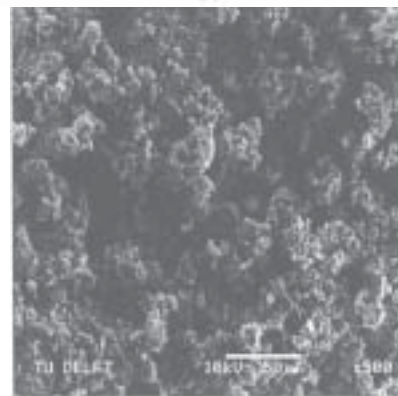
Surface morphology and texture as well as particles size of the synthesized TiO_2 were observed by SEM and TEM investigations. The SEM images obtained for synthesized TiO_2 powder are presented in figure 4.

The SEM images exhibits that samples are composed by nanoparticles agglomerate which can be seen also in electron micrograph, but clearly this agglomerate are only due to superficial interaction not to chemical one. Micrographs for TiO_2 powder obtained at 500, 700, and 800°C by means of bright field – transmission electron microscopy investigations (BF-TEM) are presented in the figure 5 a, b and respectively c.

Theses images exhibit nanoparticles dispersion with a narrow size distribution as can be seen in the inset of each



(a)

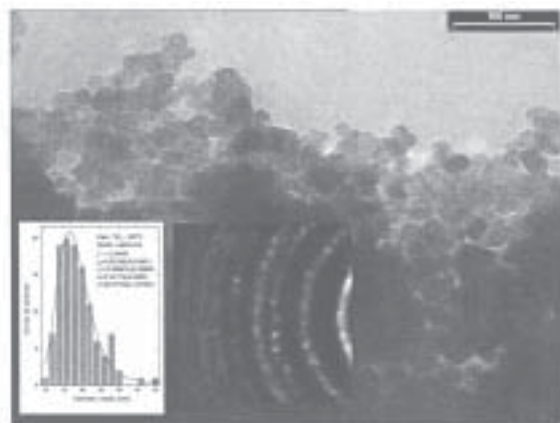


(b)

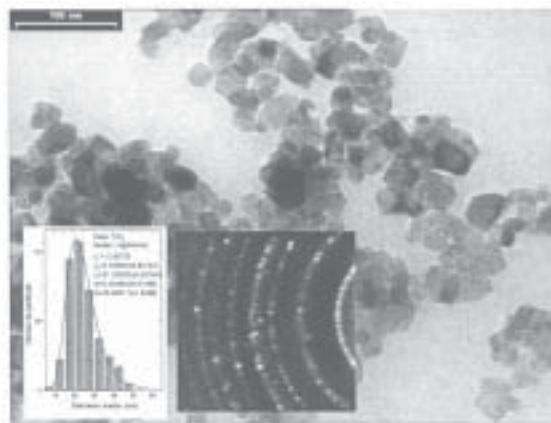
Fig. 4. SEM images of TiO_2 nanopowders obtained at: (a) 700°C and (b) 800°C

image were a histogram of area weighting diameter of nanoparticles that was fitted with log-normal function is represented. The TEM samples were deposited on 300 mesh grid form coated with 10%wt. nanoparticles in ethanol.

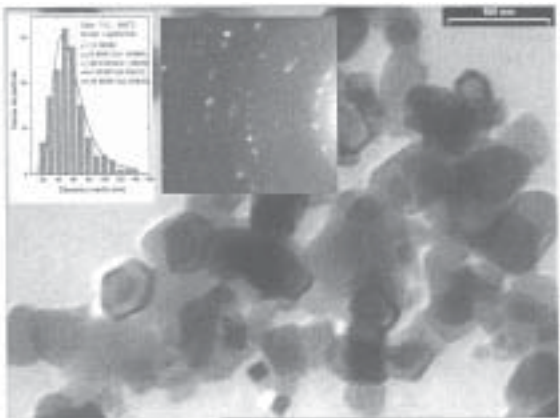
Particle has a sharp edge and narrow distribution on diameter. Values of diameter have a rising tendency over the temperature, from ~10 nm to 50 nm. The crystallinity of sample could be observed in BFTEM image by sharpe edge and square and hexagonal form of particles, and from SAED insets that show typical electron diffraction for polycrystalline material; in case of 800°C sample are obviously that specimen has larger size nanocrystals.



(a)



(b)



(c)

Measuring the rings diameters from SAED pattern and calculate planar distance, it can be confirmed that the obtained powder is anatase, with tetragonal structure included in space group $I4_1/amd$ (141) and lattice constant $a = 0.378$ nm and $c = 0.951$ nm. The location of plane (101), (103), (200) and (105), used for SAED measurement, are in good agreements with JCPDS 84-1285. SAED pattern consist in a set of ring and spot that prove the existence of crystals in powder. The width of the rings is directly connected to crystal dimension by Debye-Scherrer relation, given by:

$$D = \frac{57,3 \cdot k \cdot \lambda}{\beta \cdot \cos \theta} \quad (1)$$

where k is the shape factor of particles, β full width at half of maximum and θ Bragg angle for selected ring.

The particle diameter is evaluated by mean value of the distances between pairs of parallel tangents to the projected outline of the particle (Feret's diameter) and mean diameter is calculated assuming a lognormal distribution of experimental data [21-25]. Diameters distribution and fitting curve assume a lognormal distribution for diameter dispersion (insets fig. 5 a-c). The lognormal function used for fit the experimental curves are given by (2):

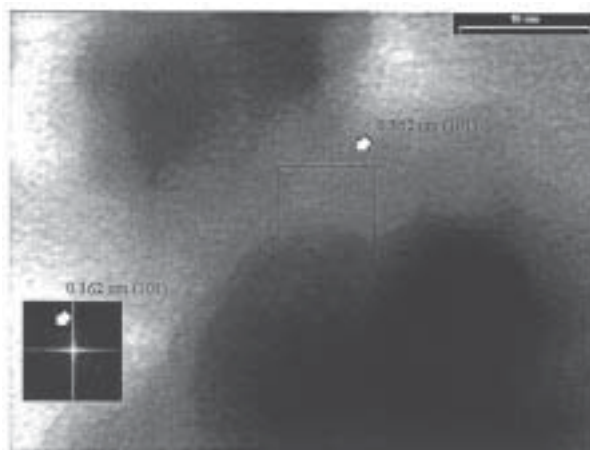
$$y = Ae^{\frac{\ln^2(x/x_c)}{2w^2}} \quad (2)$$

where A is an arbitrary constant related to particle number, x_c represent the distribution maximum and w is strong correlated with particle diameter dispersion. The samples have a narrow size distribution; only 500°C sample exhibits a second peak around 25-30 nm.

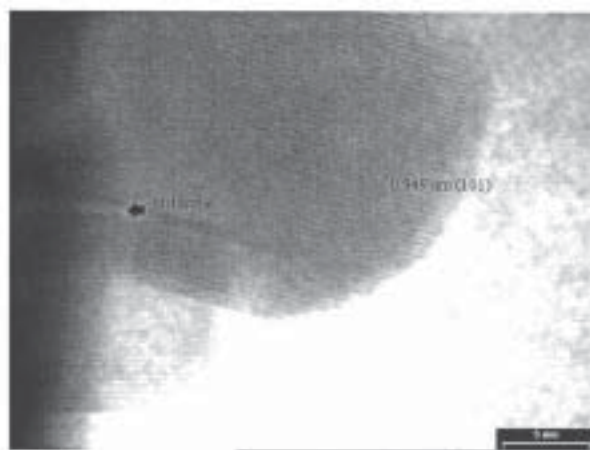
Crystals of 15 nm for 500°C, 23 nm for 700 and 800°C have been obtained. The crystals have a spherical form in the first case (500°C) and pallets form in the second and

Fig. 5. Morphology and structural characterization of TiO_2 nanopowder obtained at (a) 500°C; (b) 700°C; (c) 800°C

third case (for 700 and 800°C). This conclusion can be explained by assuming that the formation of crystals at higher temperature is due to the agglomeration of few crystals (2-10 crystals). This conclusion can be directly seen in HRTEM image mode (fig. 6) where the large crystals



(a)



(b)

Fig. 6. HRTEM images obtained for TiO_2 samples for 500°C (a), 700°C (b)

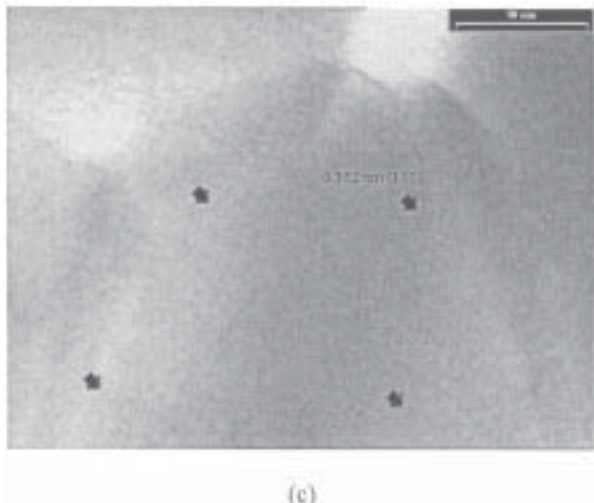


Fig.6. HRTEM images obtained for TiO_2 samples for 800°C (c),

have structural defects. The interface between crystals can be observed only in a few cases and cannot be assumed to be a sample characteristic.

Measurements were carried out by using Fourier Transform, that could be use to improve accuracy of measured data values, by modifying measuring marks form line to point. No additional phases of TiO_2 were found in the sample, so the nanopowder is stable in the anatase phase.

Conclusions

The TiO_2 powder, synthesized by thermal hydrolysis of TiCl_4 , was characterized by high-resolution transmission electron microscopy (HRTEM).

SAED pattern consist in a set of ring and spot that can prove the existence of crystals in powder.

The crystallinity of sample was observed in BFTEM image by sharp edge and square and hexagonal form of particles, and from SAED insets that show typical electron diffraction for polycrystalline material and in case of 800°C sample are obviously that specimen has larger size nanocrystals.

Crystals of 15 nm for 500°C, 23 nm for 700 and 800°C have been obtained. The crystals have a spherical form in the first case (500°C) and pallets form in the second and third case (for 700 and 800°C). This conclusion can be explained by assuming that the formation of crystals at higher temperature is due to the agglomeration of few crystals (2-10 crystals).

The studied nanopowder is stable in the anatase phase because no additional phases of TiO_2 were finding in the sample.

Acknowledgements: The experimental part of this study was possible with the support of the Socrates-Erasmus Program and of Prof. Dr. Joop Schoonman, Delft University of Technology.

References

1. TIAN Z. R., TONG W., WANG J. Y., DUAN N. G., KRISHNAN V.V., SUIB S. L., Science 276, 1997, p.926
2. NAKADE S., SAITO Y., KUBO W., KITAMURA T., WADA Y., YANAGIDA S., J. Phys. Chem. B. 107, 2003, p.8607
3. KARCH J., BIRINGER R., GLEITER H., Nature, 330, 1987, p.556
4. YIN J. B., XHAO X. P., Chem. Mater., 14, 2002, p.4633
5. HOFFMAN M. R., MARTIN S. T., CHOI W., BAHNEMANN D. W., Chem. Res., 95, 1995, p.69
6. XIAOHONG WU, JIANG ZHAOHUA, LIU HUILING, LI XUANDONG, HU XINGUO, Materials Chemistry Physics, 80, 2003, p.39
7. YUN-QIU HE, YI-HONG PING, Materials Chemistry and Physics, 78, 2003, p.614
8. CHIA-SZU FANG, YU-WEN CHEN, Materials Chemistry and Physics, 78, 2003, p.739
9. XIAO YINGHONG, WANG XIN, YANG XUJIE, LU LUDE, Materials Chemistry and Physics, 77, 2002, p.609
10. RUAN S., FENGQUIN WU, ZHANG T., Materials Chemistry and Physics, 69, 2001, p.7
11. BAORANG LI, XIAOHUI WANG, MINYU YAN, LONGTU LI, Materials Chemistry and Physics, 78, 2003, p.184
12. ZILONG TANG, JUNYING ZHANG, ZHE CHENG, ZHONGTAI ZHANG, Materials Chemistry and Physics 77, 2002, p.314
13. BU S. J., JIN Z. G., LIU X. X., YANG L. R., CHENG Z. J., Journal of the European Ceramic Society 25, 2005, p.673
14. TSUGIO SATO, YASUHIKO FUKUGAMI, Solid State Ionics, 141-142, 2001, p.397
15. WU XIAOHONG, JIANG ZHAOHUA, LIU HUILING, LI XUANDONG, HU XINGUO, Materials Chemistry and Physics, 80, 2003, p.39
16. JIAGUO YU, XIUJIAN ZHAO, QINGNAN ZHAO, Materials Chemistry and Physics, 69, 2001, p.25
17. FUJISHIMA A., HONDA K., Nature, 37, 1972, p.238
18. KAVAN L., GRATZEL M., GILBERT S. E., KLEMENTZ C., SCHEEL H. J., J. Am. Chem. Soc. 118, 1996, p.6716
19. SANG SEOK, JOO HYUN KIM, Materials Chem. Phys. 86, 2004, p.176
20. YUAN-QING LI, SHAO-YUN FU, GUO YANG, MING LI, J. Non-Crystalline Solids, 352, p.3339
21. CIUPINA V., CARAZEANU I., PRODAN G., GUGUTA C., Microchim. Acta, 147, 2004, p. 151
22. CIUPINA V., CARAZEANU I., PRODAN G., VASILE E. Balcan Physics Letters, 11, 2003,128
23. CARAZEANU POPOVICI I., GIRTU M., DUMBRAVA A. CHIRILA E., CIUPINA V., PRODAN G., Ovidius University Annals of Chemistry 17, 2006, 230
24. RAJARAM S. MANE, OH-SHIM JOO, WON JOO LEE, SUNG-HWAN HAN, Micron 38, 2007, p.85
25. CARAZEANU POPOVICI I., CHIRILA E., POPESCU V., CIUPINA V., PRODAN G., Rev. Chim. (Bucureşti), 58, nr. 8, 2007, p. 716

Manuscript received: 6.11.2007